Journal of Nanoscience and Technology 1(1) (2015) 1–3

ISSN: 2455-0191

Contents List available at JACS Directory

Journal of Nanoscience and Technology

journal homepage: www.jacsdirectory.com/jnst

Rational Synthesis of Ni Doped α-Fe_2O_3 Nanoplates and Their Uric Acid Sensing Behaviour

R. Suresh[1], K. Giribabu[2], R. Manigandan[2], A. Stephen[3], V. Narayanan[2,*]

[1]*Department of Chemistry, SRM University, Ramapuram, Chennai – 600 089, TN, India.*
[2]*Department of Inorganic Chemistry, University of Madras, Guindy Campus, Chennai – 600 025, TN, India.*
[3]*Department of Nuclear Physics, University of Madras, Guindy Campus, Chennai – 600 025, TN, India.*

ARTICLE DETAILS

Article history:
Received 19 July 2015
Accepted 21 August 2015
Available online 03 September 2015

Keywords:
Ni-Doped α-Fe_2O_3
Hydrolysis
Nanoplates
Sensor
Uric Acid

ABSTRACT

A new 15% Ni-doped α-Fe_2O_3 nanoplates modified glassy carbon electrode (GCE) was fabricated and used for the sensing of uric acid (UA). The Ni-doped α-Fe_2O_3 nanoplates were prepared by hydrolysis method. The structure and morphology of the sample was characterized by X-ray diffraction (XRD), Fourier transform infrared spectroscopy (FTIR), UV-Visible spectroscopy (UV-Vis) and field emission scanning electron microscopy (FE-SEM). The modified electrode was prepared by drop coating method. The electrochemical sensing behavior of the Ni-doped α-Fe_2O_3 modified GCE was investigated by cyclic voltammetry (CV). Ni-doped α-Fe_2O_3 modified electrode exhibits a 150 mV shift in the oxidation potential of UA in the cathodic direction with a remarkable enhancement of the current response than the bare GCE. It is much promising for the modified films to be used as an electrochemical sensor for the detection of UA.

1. Introduction

The most stable *α*-Fe_2O_3 (hematite) is an important functional semiconductor (*Eg* = 2.1 eV) which is environmentally friendly and has low toxicity. It has been the widely investigated material due to its applications in the field of photocatalyst [1, 2], solar cells [3], electrochemical sensor [4], gas sensors [5], and batteries [6] etc. Since the morphology and crystallographic forms are generally believed to be responsible for their properties [7], the controlled synthesis of Fe_2O_3 has received much interest in material research. Hence, many methods have been reported for the synthesis of α-Fe_2O_3 including forced hydrolysis [8], hydrothermal synthesis [9], microwave irradiation method [10], and combustion method [11] method etc. Among them, hydrolysis of Fe^{3+} plays an important role in natural system. This method does not need the addition of any precipitator. Doping of different metal ions or metal oxides into Fe_2O_3 will find new application or improve the performance of existing applications. For instance, Niu et al [12] found that the material mixed with rare earth oxides through a sol-gel method in citric acid system presented high gas sensitivity to gasoline. Jing et al [13] reported that the Ni-doped γ-Fe_2O_3 exhibits higher gas sensitivity and better selectivity to ethanol than the pure γ-Fe_2O_3. Recently, we have reported that the Co doped α-Fe_2O_3 exhibits higher electrochemical sensing property than the pure α-Fe_2O_3. It is noted that until now most of the researchers focused mainly on doping of metal ion into γ-Fe_2O_3, while doping of metal ion in α-Fe_2O_3 and their electrochemical sensing properties have rarely reported. In this regard, we prepared Ni-doped α-Fe_2O_3 nanoplates as a voltammetric sensor for UA. In general, selective and accurate determination of UA is essential in clinical analysis. Hence, enzyme-based UA sensors were developed, but the enzymes were expensive and difficult to handle. Also, enzymes based UA sensor did not have long-term stability due to their inherent instability. On the contrary, Ni-doped α-Fe_2O_3 nanoplates could be an excellent substitute for enzymes.

Here, we fabricated a new voltammetric sensor with Ni-doped α-Fe_2O_3 nanoplates to test whether Ni-doped α-Fe_2O_3 nanoplates could efficiently detect UA. The sensor material was prepared by simple hydrolysis method and was characterized with XRD, FT-IR, UV–vis spectrum, and FE-SEM.

2. Experimental Methods

2.1 Materials

Ferric chloride ($FeCl_3$), nickel acetate and potassium chloride were purchased from Qualigens. Uric acid was purchased from Sigma. The above chemicals were used as received. Doubly distilled water was used as the solvent.

2.2 Sample Preparation

In order to prepare Ni-doped α-Fe_2O_3, $Ni(CH_3COO)_2{\cdot}6H_2O$ salt was added to the aqueous solution of $FeCl_3$. The mole ratio of Ni and Fe was 15:85. The solutions were refluxed in a water bath for 16 h. The obtained yellow powders (Ni-doped FeOOH) were calcined at 600 °C for 6 h to get reddish brown, 15% Ni-doped α-Fe_2O_3 nanostructures.

2.3 Characterization

The structure of the sample was analyzed by a Rich Siefert 3000 diffractometer with Cu-Kα_1 radiation (λ = 1.5406 Å). FTIR spectrum of the sample was recorded by using a Schimadzu FT-IR 8300 series instrument. The UV–Vis absorption spectrum was obtained on a CARY 5E UV–vis-NIR spectrophotometer. The morphology and size was analyzed by FE-SEM using HITACHI SU6600 field emission-scanning electron microscopy. The BET surface area was measured using a Micromeritics (ASAP 2020) analyzer. The electrochemical experiments were performed on a CHI 600A electrochemical instrument using the as-modified electrodes and bare GCE as working electrode, a platinum wire was the counter electrode and saturated calomel electrode (SCE) was the reference electrode.

2.4 UA Sensor Fabrication

Ni-doped α-Fe_2O_3 dispersion (1 mg of sample in 5 mL of acetone) was prepared by using ultrasonication method. Highly polished GCE was coated with 5 µL of Ni-doped α-Fe_2O_3 dispersion. The modified electrode was activated in 0.1 M KCl solution by successive cyclic scans between -0.2 and +0.6 V. Before and after each experiment, the modified electrode was washed with distilled water and reactivated by the method mentioned above.

*Corresponding Author
Email Address: vnnara@yahoo.co.in (V. Narayanan)

Cite this Article as: R. Suresh, K. Giribabu, R. Manigandan, A. Stephen, V. Narayanan, Rational synthesis of Ni doped α-Fe_2O_3 nanoplates and their uric acid sensing behaviour, J. Nanosci. Tech. 1(3) (2015) 1–3.

3. Results and Discussion

3.1 XRD analysis

Fig. 1 represents the powder XRD pattern of α-Fe_2O_3 (15% Ni). The diffraction pattern of α-Fe_2O_3 (15% Ni) was similar to that of pure α-Fe_2O_3 (not shown here) and closely matched with the standard α-Fe_2O_3 reflections (JCPDS No. 882359). α-Fe_2O_3 (15% Ni) has an orthorhombic structure. Nickel dopant did not exist as nickel oxide in the doped sample. However, the diffraction peaks of the Ni-doped sample are different from that of pure α-Fe_2O_3 in relative intensity, which probably results from the incorporation of nickel atom into the Fe_2O_3 lattice, because of the ionic radius of the Ni^{2+} (0.78 Å) is similar to that of Fe^{3+} (0.69 Å). In addition, all the diffraction peaks of α-Fe_2O_3 (15% Ni) are slightly shifted to higher 2θ values than that of pure α-Fe_2O_3. These results suggest that the Ni^{2+} is well dissolved within the Fe_2O_3 lattice. Further, the diffraction peaks of the samples show broadening indicating the ultrafine nature of the particles. On the basis of Scherrer's equation, the average crystallite size was estimated by applying peak broadening analysis to hematite (32.8°) diffractions. The average crystallite size is calculated as 49 nm for α-Fe_2O_3 and 34 nm for α-Fe_2O_3 (15% Ni). The results suggests that the crystallite size of α-Fe_2O_3 (15% Ni) turns smaller, which means that the addition of Ni^{2+} can effectively decreases the crystalline grain growth. This result is consistent with the reports in which the added Ni decreases the crystallite grain growth of γ-Fe_2O_3 [13].

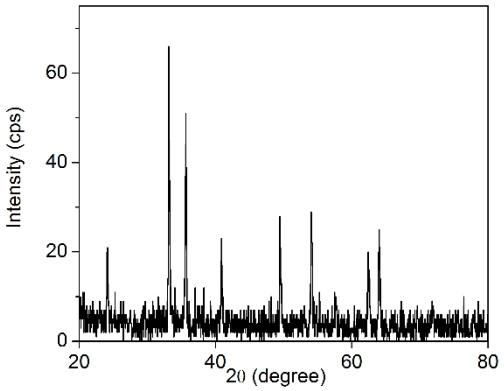

Fig. 1 XRD pattern of α-Fe_2O_3 (15% Ni)

3.2 FT-IR Analysis

FT-IR spectrum of α-Fe_2O_3 (15% Ni) is similar to that of pure α-Fe_2O_3 and is shown in Fig. 2. The characteristic bands at 3401, 1621, 556, and 447 cm^{-1} were observed in Fig. 2. The band associated with the lattice water molecule is broad, and is observed in a region of 3401 cm^{-1} and 1621 cm^{-1}. The simultaneous presence of these two bands indicates that, the water of crystallization is present in the sample. Huo et al [15] claimed the bands of 556 cm^{-1} and 447 cm^{-1} are due to Fe-O vibrational mode of α-Fe_2O_3. In Ni doped sample, the Fe-O stretching vibrational mode is observed in 555 cm^{-1} and 460 cm^{-1} which assures the hematite phase [16].

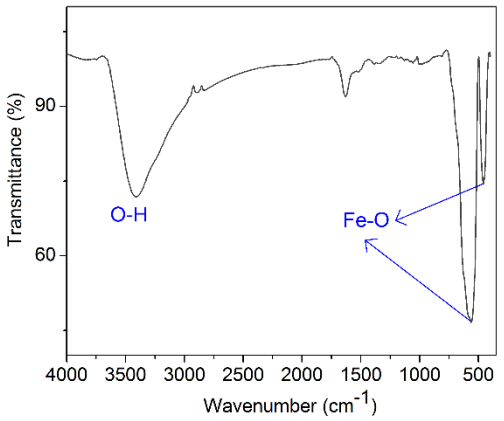

Fig. 2 FTIR spectrum of α-Fe_2O_3 (15% Ni) nanoplates

3.3 UV-Visible Analysis

The UV-visible absorption spectrum of α-Fe_2O_3 (15% Ni) nanoplates (Fig. 3) shows three absorption bands at around 350, 536 and 674 nm. The absorption band present in the region of 400-600 nm can be assigned to $^6A_1 \rightarrow {}^4T_2$ (^4G), d-d transition of Fe^{3+} as well as the pair excitations, $^6A_1 + {}^6A_1 \rightarrow {}^4T_2$ (^4G) + $^4T_2$ (^4G) of two adjacent Fe^{3+} cations ($^6A_1$ and $^4T_2$ (^4G)), referred to as the ground state and first excited state configuration of high spin Fe^{3+}, respectively. Also, the band at 350 nm is mainly results from the ligand to metal charge- transfer transitions and partly from the contributions of the Fe^{3+} ligand-field transition $^6A_1 \rightarrow {}^4T_2$ (^4D) [17]. Inset in Fig. 3 shows the plot of $(\alpha h\nu)^2$ versus $h\nu$ for the α-Fe_2O_3 (15% Ni) nanoplates. The estimated band gap of the sample is found to be 2.02 eV for α-Fe_2O_3 (15% Ni) which is in good agreement with a band gap value of α-Fe_2O_3 [18]. The steep absorption edge in α-Fe_2O_3 (15% Ni) nanoplates is indicative of the uniform particle morphology and size with fairly good crystallinity [19].

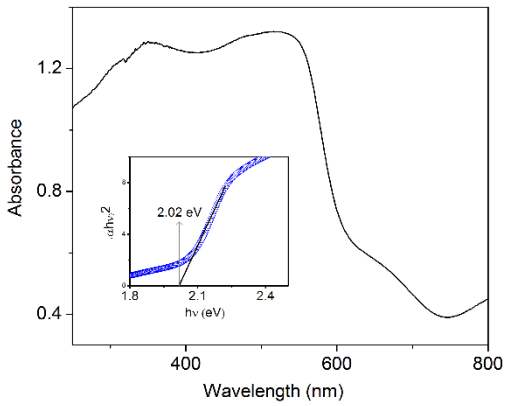

Fig. 3 UV-Visible absorption spectrum of α-Fe_2O_3 (15% Ni)

3.4 FE-SEM Analysis

Fig. 4 shows the SEM (image a-b) and FE-SEM images (image c-d) of α-Fe_2O_3 (15% Ni). From the Fig. 4, it can be seen that the α-Fe_2O_3 (15% Ni) particles has elongated plate-like shape with the widths of 69 nm and lengths up to 263 nm. It should be mentioned that the particle shape of the α-Fe_2O_3 (15% Ni) is altered in comparison with the morphology of pure α-Fe_2O_3 which has sphere-like morphology. Therefore the addition of $Ni(CH_3COO)_2{\cdot}6H_2O$ has vital role in the formation of nanoplates.

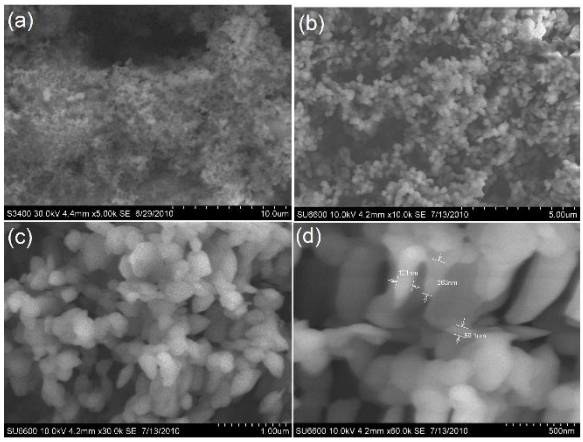

Fig. 4 SEM images (a, b), FE-SEM images (c, d) and EDS of α-Fe_2O_3 (15% Ni) nanoplates

3.5 BET Analysis

BET analysis was performed to determine the surface area of α-Fe_2O_3 (15% Ni) nanoplates. In order to get sample with surface area, we should use lower concentration of precursor salt and lower reaction temperature. The concentration we used here is 0.5 M with higher calcination temperature than the reported values [20]. The surface area of the α-Fe_2O_3 is 4.95 m^2g^{-1} whereas the surface area of the α-Fe_2O_3 (15% Ni) is 5.56 m^2g^{-1}. These results showed that the addition of 15% Ni increased the surface area of the sample.

3.6 Electrocatalytic Property

UA sensing behaviour of α-Fe_2O_3 (15% Ni) nanoplates were examined by cyclic voltammetry. Fig. 5 shows the cyclic voltammogram of 4 mM UA in 0.1 M KCl at bare, α-Fe_2O_3, and α-Fe_2O_3 (15% Ni) nanoplates modified GCE along with bare GCE. Bare GCE (Inset in Fig. 5) shows a very broad peak at about +0.42 V for the oxidation of UA. Noticeably, voltammogram of UA at α-Fe_2O_3 (5-20% Ni) modified GCE showed higher oxidation peak

current with lower oxidation potential at +0.3 V and a small re-reduction peak at +0.18 V. The overpotential had thus decreased by +0.13 V. This result indicates the enhanced UA sensing ability of α-Fe_2O_3 (15% Ni) modified electrode. This UA oxidation potential is comparable or better than the previously reported values [21-23]. Generally, the oxidation of UA is irreversible at GCE [24]. However, α-Fe_2O_3 (15% Ni) modified GCE shows re-reduction peak of UA which has not been reported in most of the literature [23], showing the increased reaction reversibility at the α-Fe_2O_3 (15% Ni) modified GCE. This electrocatalytic effect was attributed to the larger available surface area of α-Fe_2O_3 (15% Ni) nanoplates as evidenced from FE-SEM and BET analysis.

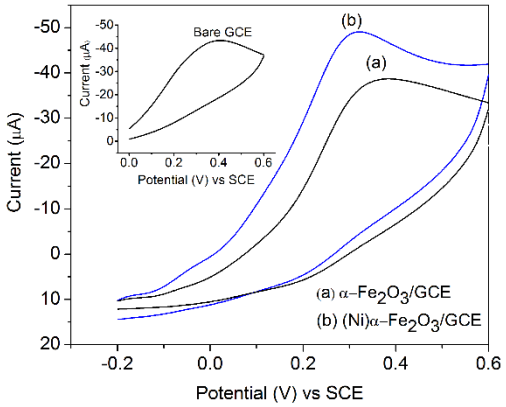

Fig. 5 Cyclic voltammetric response of 4 mM UA at (a) pure α-Fe_2O_3/GCE and (b) α-Fe_2O_3 (15% Ni)/GCE. Inset Figure: Cyclic voltammetric response of 4 mM UA at bare GCE. Scan rate: 50 mV/s

4. Conclusion

In summary, Ni-doped α-Fe_2O_3 nanoplates were successfully prepared by hydrolysis method. The XRD, FTIR and UV-visible studies confirms the formation of the sample. The FE-SEM of α-Fe_2O_3 (15% Ni) shows that the particles were nanoplates liked shape. The electrochemical sensing properties of these nanoparticles were investigated. α-Fe_2O_3 (15% Ni) modified GCE exhibited higher anodic current response for 4 mM UA than the bare GCE with shifts in potential.

Acknowledgement

One of the author (RS) acknowledges the CSIR, New Delhi, for the financial assistance in the form of Senior Research Fellowship. We acknowledge the FE-SEM facility provided by the National Centre for Nanoscience and Nanotechnology, University of Madras.

References

[1] D. Wodka, R.P. Socha, E. Bielanska, M.E. Wodka, P. Nowak, P. Warszynski, Photocatalytic activity of titanium dioxide modified by Fe_2O_3 nanoparticles, App. Sur. Sci. 319 (2014) 173–180.

[2] S.W. Cao, Y.J. Zhu, G.F. Cheng, Y.H. Huang, Preparation and photocatalytic property of α-Fe_2O_3 hollow core/shell hierarchical nanostructures, J. Phys. Chem. Solids. 71 (2010) 1680-1683.

[3] S. S. Shinde, R. A. Bansode, C. H. Bhosale, K.Y. Rajpure, Physical properties of hematite α-Fe_2O_3 thin films: application to photoelectrochemical solar cells, J. Semicond. 32 (2011) 013001.

[4] R. Suresh, R. Prabu, A. Vijayaraj, K. Giribabu, A. Stephen, V. Narayanan, fabrication of α-Fe_2O_3 nanoparticles for the electrochemical detection of uric acid, Synth. React. Inorg. Metal-Org. nano-Met. Chem. 42 (2012) 303-307.

[5] W. Jin, B. Dong, W. Chen, C. Zhao, L. Mai, Y. Dai, synthesis and gas sensing properties of Fe_2O_3 nanoparticles activated V_2O_5 nanotubes, Sens. Actuators. B.145 (2010) 211–215.

[6] N.K. Chaudharia, M.S. Kima, T.S. Baeb, J.S. Yua, Hematite (α-Fe_2O_3) nanoparticles on vulcan carbon as an ultra-high capacity anode material in lithium ion battery, Electrochim. Acta. 114 (2013) 60– 67.

[7] R. Zysler, Size Dependence of the Spin-Flop Transition in Hematite Nanoparticles, Phys. Rev. B. 68 (2003) 212408.

[8] M. Chen, J. Jiang, X. Zhou, G. Diao, preparation of akaganeite nanorods and their transformation to sphere shape hematite, J. Nanosci. Nanotechnol. 8 (2008) 3942-3948.

[9] C.S. Bijua, D.H. Rajab, D.P. Padiyana, Glycine assisted hydrothermal synthesis of α-fe_2o_3 nanoparticles and its size dependent properties, Chem. Phys. Lett. 610–611 (2014) 103–107.

[10] N. Kijima, M. Yoshinaga, J. Awaka, J. Akimoto, Microwave synthesis, characterization, and electrochemical properties of α-Fe_2O_3 nanoparticles, Solid State Ionics. 192 (2011) 293–297.

[11] R. Ianos, E.A. Taculescu (Moaca), C. Pacurariu, D. Niznansky, γ-Fe_2O_3 nanoparticles prepared by combustion synthesis, followed by chemical oxidation of residual carbon with H_2O_2, Mat. Chem. Phy. 148 (2014) 705 – 711.

[12] X.S. Niu, W.M. Du, W.P. Du, Preparation, characterization and gas-sensing properties of rare earth mixed oxides, Sens. Actuators B Chem. 99 (2004) 399-404.

[13] Z. Jing, Fabrication and gas sensing properties of Ni-doped gamma-Fe_2O_3 by anhydrous solvent method, Mat. Let. 60 (2006) 3315-3318.

[14] R. Suresh, R. Prabu, A. Vijayaraj, K. Giribabu, A. Stephen, V. Narayanan, Facile synthesis of cobalt doped hematite nanospheres: magnetic and their electrochemical sensing properties, Mater. Chem. Phys. 134 (2012) 590-596.

[15] L. Huo, Q. Li, H. Zhao, L. Yu, S. Gao, J. Zhao, Sol–gel route to pseudocubic shaped α-Fe_2O_3 alcohol sensor: preparation and characterization, Sens. Actuators B. 107 (2005) 915–920.

[16] R. Suresh, K. Giribabu, R. Manigandan, A. Vijayaraj, R. Prabu, A. Stephen, V. Narayanan, α-Fe_2O_3 nanoflowers: Synthesis, characterization, electrochemical sensing and photocatalytic property, J. Iran. Chem. Soc. 11 (2014) 645–652.

[17] T. Hashimoto, T. Yamada, T. Yoko, Third-order nonlinear optical properties of sol–gel derived α-Fe_2O_3, γ-Fe_2O_3, and Fe_3O_4 thin films, J. Appl. Phys. 80 (1996) 3184-3190.

[18] W.B.J. Ingler, S.U.M. Khan, Photoresponse of spray pyrolytically synthesized copper-doped p-Fe_2O_3 thin film electrodes in water splitting, Int. J. Hydrogen Energ. 30 (2005) 821-827.

[19] H.I. Hsiang, F.S. Yen, Effects of mechanical treatment on phase transformation and sintering of nano-sized γ-fe_2o_3 powder, Ceram. Int. 29 (2003) 1- 6.

[20] G. Goloverda, B. Jackson, C. Kidd, V. Kolesnichenko, Synthesis of ultrasmall magnetic iron oxide nanoparticles and study of their colloid and surface chemistry, J. Magn. Magn. Mater. 321 (2009) 1372–1376.

[21] Y. Zhao, J. Bai, L. Wang, X. Hong, P. Huang, H. Wang, L. Zhang, Simultaneous electrochemical determination of uric acid and ascorbic acid using L-cysteine self-assembled gold electrode, Int. J. Electrochem. Sci. 1 (2006) 363-371.

[22] Y. Li, X. Lin, Simultaneous electroanalysis of dopamine, ascorbic acid and uric acid by poly (vinyl alcohol) covalently modified glassy carbon electrode, Sens. Actuators. B 115 (2006) 134-139.

[23] L. Wang, P. Huang, J. Bai, H. Wang, X. Wu, Y. Zhao, Voltammetric sensing of uric acid and ascorbic acid with poly(*p*-toluene sulfonic acid) modified electrode, Int. J. Electrochem. Sci. 1 (2006) 334-342.

[24] J. L. Owens, H.A.J. Marsh, G. Dryhurst, Electrochemical oxidation of uric acid and xanthine: An investigation by cyclic voltammetry, double potential step chronoamperometry and thinlayer spectroelectrochemistry, J. Electroanal. Chem. 91 (1978) 231-247.